Diffusion, annihilation, and chemical reactions in complex networks with spatial constraints

Thorsten Emmerich,[1] Armin Bunde,[1] and Shlomo Havlin[2]
[1]*Institut für Theoretische Physik, Justus-Liebig-Universität Giessen, 35392 Giessen, Germany*
[2]*Minerva Center and Department of Physics, Bar-Ilan University, Ramat-Gan 52900, Israel*
(Received 16 July 2012; published 10 October 2012)

We consider Erdös-Rényi–type networks embedded in one-dimensional ($d_e = 1$) and two-dimensional ($d_e = 2$) Euclidean space with the link-length distribution $p(r) \sim r^{-\delta}$. The dimension d of these networks, as a function of δ, has been studied earlier and has been shown to depend on δ. Here we consider diffusion, annihilation, and chemical reaction processes on these spatially constrained networks and show that their dynamics is controlled by the dimension d of the system. We study, as a function of the exponent δ and the embedding dimension d_e, the average distance $\langle r \rangle \sim t^{1/d_w}$ a random walker has traveled after t time steps as well as the probability of the random walker's return to the origin $P_0(t)$. From these quantities we determine the network dimension d and the dimension d_w of the random walk as a function of δ. We find that the fraction d/d_w governs the number of survivors as a function of time t in the annihilation process ($A + A \to 0$) and in the chemical reaction process ($A + B \to 0$), showing that the relations derived for ordered and disordered lattices with short-range links remain valid also in the case of complex embedded networks with long-range links.

DOI: 10.1103/PhysRevE.86.046103 PACS number(s): 89.75.Da, 05.10.Ln

I. INTRODUCTION

A large number of complex networks are embedded in Euclidean space and, thus, are subject to spatial constraints. Examples range from transportation networks like the global airline network via the Internet to social networks like cellular phones and author networks [1–13]. In recent papers [14–17], these kinds of networks were modeled by Erdös-Rényi (ER) [18–20] or Barabási-Albert networks [1,2] that are embedded in Euclidean space with a link length distribution that follows a power law, $p(r) \sim r^{-\delta}$. The results indicated that the dimension of these networks [16,17] as well as their topological properties [14] change continuously with δ. For δ below the embedding dimension d_e, the dimension of the network can be regarded as infinite, and the topological properties such as the dependence of the mean topological length on the system size are the same as those for $\delta = 0$. For δ above $2d_e$ the spatial constraints are strong and the network behaves like a regular lattice with dimension d_e. In the intermediate δ range between d_e and $2d_e$, the dimension of the embedded network changes continuously from $d = \infty$ to $d = d_e$ [16,17].

The knowledge of the dimension of a system is crucial for characterizing its physical properties, such as diffusion and phase transitions on the structure. In this paper we test if and how the dimension of the embedded network determines dynamical processes on networks such as the diffusion-driven annihilation of identical particles and the diffusion-driven chemical reactions of two kinds of particles. It is known that, in regular lattices, in both kinds of processes the ratio between the lattice dimension d and the dimension d_w of the random walk on that lattice (usually $d_w = 2$) plays a crucial role [21–25]. For the annihilation process in regular lattices, the concentration of surviving particles decays as $c(t) \sim t^{-d/d_w}$ as long as $d/d_w < 1$ and as $c(t) \sim 1/t$ for $d/d_w \geqslant 1$ [24,26]. For the chemical reaction between two species of particles which initially are randomly distributed over the lattice with the same concentration, the concentration of surviving particles decays as $c(t) \sim t^{-d/2d_w}$ as long as $d/d_w < 2$ and as $c(t) \sim 1/t$ for $d/d_w \geqslant 2$ [24,26]. For chemical reactions on Barabási-Albert networks not embedded in Euclidean space, a faster decay is also possible [27,28].

In this paper, we focus on Erdös-Rényi–type networks embedded in d_e dimensional space with a power-law distribution of the link lengths and study (a) diffusion (Sec. III), (b) diffusion-driven annihilation (Sec. IV), and (c) diffusion-driven chemical reactions (Sec. V). We study the ratio d/d_w as a function of δ and d_e and show that the relations derived for regular lattices [Eq. (6)] remain valid when the dimension d of the embedded networks and the random-walk exponent $1/d_w$ are inserted in the relation derived for regular lattices.

We like to note that, conceptually, our model is related to the small-world network introduced by Kleinberg [29], where an underlying lattice structure is assumed and a certain fraction of long-range connections (with length taken from a power-law distribution) is added. In our model, no such underlying structure exists, and the ratio between "short" and "long" connections is solely controlled by the spatial exponent δ and the system size.

II. GENERATION OF THE NETWORKS

The nodes of the network are located at the sites of a d_e-dimensional regular lattice, either a linear chain of length L ($d_e = 1$) or a square lattice of size $L \times L$ ($d_e = 2$). We assign to each node a fixed number k of links (in most cases, $k = 4$). Actually, this network is a random regular network since all links have the same degree. It is expected (and we have also verified it numerically) that random regular networks and ER networks with the same spatial constraints are in the same universality class.

To generate the spatially embedded networks, we use the following iterative algorithm: (i) We pick a node i randomly and choose, for one of its available k_i links, a distance $r (1 \leqslant r \leqslant L)$ from the given probability distribution $p(r) \sim r^{-\delta}$. It is easy to see that the distance r can be obtained from random numbers $0 < u \leqslant 1$ chosen from the unit distribution

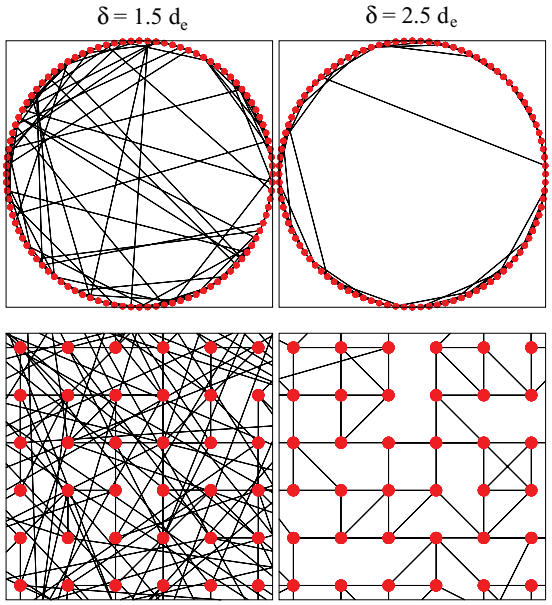

FIG. 1. (Color online) Illustration of ER networks embedded in linear chains (top) and embedded in square lattices (bottom) for $\delta = 1.5d_e$ and $2.5d_e$.

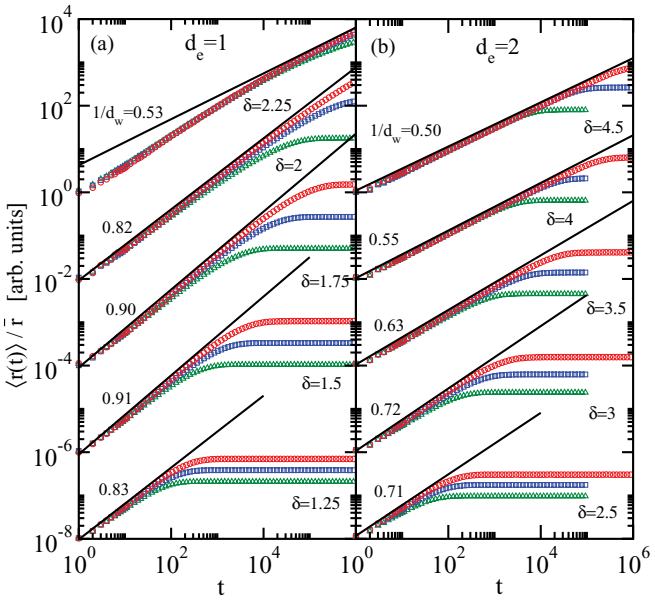

FIG. 2. (Color online) The average distance $r \equiv \langle r(t)\rangle$ of a diffusing particle from its starting site as function of time t for ER networks with $k = 4$ embedded (a) in linear chains ($d_e = 1$) of length $L = 10^5$(green triangle), 10^6(blue square), and 10^7(red circle) and (b) in square lattices ($d_e = 2$) of length $L = 3 \times 10^2$(green triangle), 10^3(blue square), and 3×10^3(red circle). The spatial exponents are $\delta = 1.25d_e$, $1.5d_e$, $1.75d_e$, $2d_e$, and $2.25d_e$. For each parameter set we averaged over 50 configurations. The straight lines are best fits to the data with slope $1/d_w$. For transparency, the four lower plots in each panel have been shifted vertically by 10^{-2} to 10^{-8}.

by

$$r = \begin{cases} [1 - u(1 - L^{d_e-\delta})]^{\frac{1}{d_e-\delta}}, & \delta \neq d_e \\ L^u, & \delta = d_e \end{cases}. \qquad (1)$$

(ii) We consider all N_r nodes between distance $r - \Delta r$ and r from node i that are not yet connected to node i. Without loss of generality, we choose $\Delta r = 1$ for the linear chain and $\Delta r = 0.4$ for the square lattice. (iii) We pick randomly one of these nodes j. If node j has at least one available link, we connect it with node i. If not, we do not connect it. Then we return to (i) and proceed with another randomly chosen node. At each step of the process, either two or no links are added. For generating the network, we have typically performed $10^3 \times L^{d_e}$ trials. Due to the generation process, the nodes of the final network do not all have exactly the same degree, but the degree follows a narrow distribution with a mean $\bar{k}$ slightly below $k = 4$ [17]. Figure 1 illustrates the ER networks embedded in $d_e = 1$ and $d_e = 2$ for $\delta = 1.5d_e$ and $2.5d_e$.

III. DIFFUSION

We assume that the diffusing particles (random walkers) are located at the nodes of the networks and can jump between linked nodes. In one time step one jump occurs, irrespective of the jump length. Using Monte Carlo simulations we have determined the mean distance $\langle r(t)\rangle$ (defined as $\langle |r(t)|\rangle$) of a diffusing particle from its starting point as a function of the number of time steps t, as well as the probability $P_0(t)$ that the random walker, after t time steps, has returned to its starting point. The random walks are on ER networks embedded in a linear chain ($d_e = 1$) and in a square lattice ($d_e = 2$). The number of nodes $N = L^{d_e}$ is 10^7 for $d_e = 1$ and 9×10^6 in $d_e = 2$, but for estimating finite-size effects we also considered smaller systems. To minimize the finite-size effects, we place the starting points of the particles inside a circle of radius $L/10$ around the center of the considered lattice. To obtain $\langle r(t)\rangle$ and $P_0(t)$, we have typically considered 10^4 random walks on each network and averaged over 50 networks for each set of parameters. For determining $P_0(t)$, we have enumerated the fraction of random walkers that, after t time steps, are back at their starting node. Figure 2 shows $\langle r(t)\rangle$ for ER networks embedded in $d_e = 1$ (a) and $d_e = 2$ (b), respectively, for δ values in the intermediate regime $d_e < \delta < 2d_e$, as well as for $\delta = 2d_e$ and $2.25d_e$, for three system sizes. For convenience, we show $\langle r(t)\rangle$ in units of the mean jump distance $\bar{r}$, which is identical to the first moment of the link length distribution $p(r)$. The figures show that, in all cases considered here, $\langle r(t)\rangle$ scales with t as a power law,

$$\langle r(t)\rangle \sim t^{1/d_w}, \qquad (2)$$

where $1/d_w$ is the diffusion exponent (d_w is sometimes called the "fractal dimension of the random walk") [30]. For $\delta < d_e$, we do not expect power-law behavior. By definition, $\langle r(t)\rangle$ is bounded between $\langle r(1)\rangle = \bar{r}$ and $\langle r(\infty)\rangle \sim L$. For $\delta < d_e$, the mean distance $\bar{r}$ is proportional to L and, hence, $\langle r(t)\rangle \sim L$. Thus, an increase of $\langle r(t)\rangle$ by a power law is not possible in this regime and we expect only logarithmic dependencies. In the regime $d_e < \delta < d_e + 1$, the mean distance $\bar{r}$ scales as

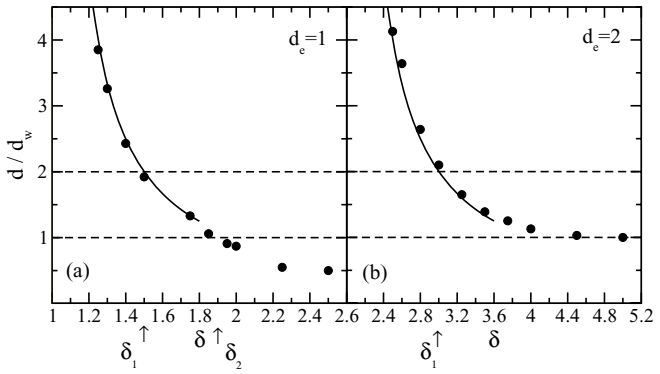

FIG. 3. The ratio of the network dimension d and the fractal dimension of the random walk d_w as a function of the spatial exponent δ for (a) $d_e = 1$ and (b) $d_e = 2$. The continuous lines are the fit from Eq. (4). For the exponents δ_1 and δ_2, d/d_w obtains the values 2 and 1, respectively.

$\bar{r} \sim L^{d_e+1-\delta}$ [14], implying that $\langle r(\infty)\rangle/\langle r(1)\rangle \sim L^{\delta-d_e}$ is large only for very large L values. Accordingly, we expect strong finite-size effects in this regime, in particular for δ close to d_e. Figure 2 shows that this is indeed the case. With increasing δ, the finite-size effects become weaker. The diffusion exponent $1/d_w$ (the slope in the double logarithmic plots) shows a slight maximum around $\delta = 1.5d_e$, but we cannot exclude the possibility that this is a finite-size effect. For $\delta = 2d_e$, the diffusion exponent is $1/d_w = 0.82$ in $d_e = 1$ and already close to 0.5, $1/d_w = 0.55$, in $d_e = 2$. For $\delta > 2d_e$, we find $1/d_w \cong 1/2$ asymptotically, as expected for regular lattices [31], but there is a strong finite-size effect in $d_e = 1$.

Note that, due to the the long-range links, the diffusion is fast with $d_w < 2$ in Eq. (2) for $\delta \leqslant 2d_e$. This is in contrast to the slow diffusion, due to obstacles, in fractals where $d_w > 2$ [24,25,30,31]. The fast diffusion is typical to Levy flights and walks which do not consider moving on a network structure, see Refs. [32–34].

Next we consider the probability of returning to the origin, $P_0(t)$. We have shown recently that $P_0(t)$ scales as $\langle r(t)\rangle^{-d}$, where d is the dimension of the embedded network [16,17]. For the networks considered in Fig. 2, we have shown earlier [17] that in $d_e = 1$ the dimensions are $d = 4.64, 2.12, 1.48, 1.07$, and 1.04 for $\delta = 1.25, 1.5, 1.75, 2$ and 2.25, respectively. In $d_e = 2$, the dimensions are $d = 5.82, 2.91, 2.21, 2.05$, and 2.02, for $\delta = 2.5, 3, 3.5, 4$, and 4.5, respectively [17]. We expect, therefore, that $P_0(t)$ decays as

$$P_0(t) \sim t^{-d/d_w}, \tag{3}$$

with d_w taken from Figs. 2(a) and 2(b). Figure 3 summarizes our results for d/d_w in $d_e = 1$ [Fig. 3(a)] and $d_e = 2$ [Fig. 3(b)]. One can see that in the intermediate δ regime, the dependence of d/d_w on δ/d_e is nearly the same in both $d_e = 1$ and 2, except for δ close to $2d_e$. The continuous curves in Figs. 3(a) and 3(b) can be well approximated (close to d_e) by

$$d/d_w = \frac{d_e}{\delta - d_e}. \tag{4}$$

Figure 4 shows $P_0(t)$ as a function of t for the same δ values as in Fig. 2. In the double-logarithmic presentation, the slopes of the straight lines are identical to d/d_w from Fig. 3. Figure 4 shows that the straight lines perfectly describe the asymptotic behavior of $P_0(t)$, i.e., $P_0(t)$ indeed scales in the anticipated way. Next we consider diffusion-driven annihilation on the spatially constrained networks.

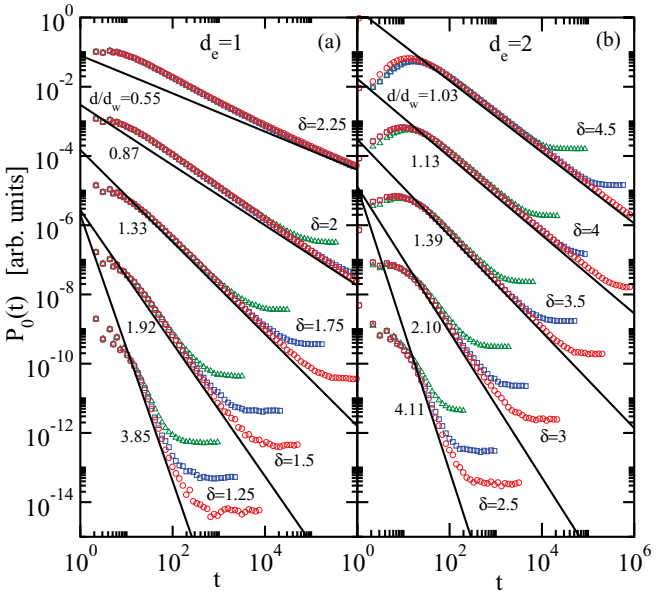

FIG. 4. (Color online) The probability of return to the origin P_0 as function of time t for the same networks as in Fig. 2. The left panel shows the results for $d_e = 1$ and the right panel for $d_e = 2$. For each parameter set we averaged over 50 configurations. The slopes of the straight lines have been taken from Fig. 3. For transparency, the four lower plots in each panel have been shifted vertically by 10^{-2} to 10^{-8}.

IV. ANNIHILATION

We study the one-species-annihilation process (see, e.g., Ref. [24]) where particles of the same species A diffuse on the network and annihilate on encounter, according to the reaction scheme

$$A + A \to 0. \tag{5}$$

We assume that, initially, at time $t = 0$, the network is fully occupied by A particles, i.e., their concentration $c(t = 0)$ is equal to 1. We are interested in the decay of $c(t)$ with time. The long-time behavior of $c(t)$ may be inferred from the following scaling argument (for regular lattices, see Ref. [24] and literature therein): Suppose that the process takes place in a container of dimensionality d. If $d \leqslant d_w$, diffusion is recurrent and a particle with $\langle r(t)\rangle \sim t^{1/d_w}$ sweeps compactly the volume $S(t) \sim \langle r(t)\rangle^d$. Consequently, after t time steps almost all particles within that volume have been annihilated, leaving behind few particles (of the order of 1). Accordingly, the concentration has decayed as

$$c(t) \sim \langle r(t)\rangle^{-d} \sim t^{-d/d_w}, \tag{6}$$

and the rate of decay depends on both d_w and the dimension d of the network. For $d > d_w$, on the other hand, the volume swept by a diffusing particle is no longer compact and the above argument does not hold. Instead, $S(t) \sim t$ and a particle is constantly exploring mostly new territory. Thus, in close analogy to the situation in regular lattices [24], one

can show that, in this case, $c(t) \sim S(t)^{-1}$ does not depend on the dimension and decays as $c(t) \sim 1/t$. Thus, it follows that the concentration $c(t)$ of the A particles should decay with time t as

$$c(t) \sim \begin{cases} t^{-d/d_w}, & d/d_w < 1 \\ t^{-1}, & d/d_w > 1 \end{cases}. \tag{7}$$

Accordingly, we can read from Fig. 3 how $c(t)$ decays with time t. For ER networks embedded in $d_e = 2$, we have $d \geqslant d_e = 2$ and $d_w \leqslant 2$. Thus, $d/d_w \geqslant 1$, and we expect $c(t) \sim t^{-1}$ for all δ values. We have confirmed numerically that this is the case. For ER networks embedded in $d_e = 1$, Fig. 3 shows that $d/d_w = 1$ for $\delta = \delta_2 \cong 1.85$. So we expect that $c(t)$ changes from $c(t) \sim t^{-1}$ for $\delta < \delta_2$ to $c(t) \sim t^{-d/d_w}$ for $\delta > \delta_2$. Figure 5 shows, in a double logarithmic presentation, $c(t)$ for $\delta = 1.85, 1.90, 1.95, 2, 2.25$, and 2.5. The straight lines are linear fits to the data with slope d/d_w taken from Fig. 3. The figure shows that the numerical results are in excellent agreement with the prediction, Eq. (7) and Fig. 3. Next we consider chemical reactions on the spatially constrained networks.

V. CHEMICAL REACTIONS

We consider A and B particles randomly distributed on the network, with the same initial concentration $c_A(0) = c_B(0)$. All particles diffuse on the network and react on encounter, according to the reaction scheme

$$A + B \to C, \tag{8}$$

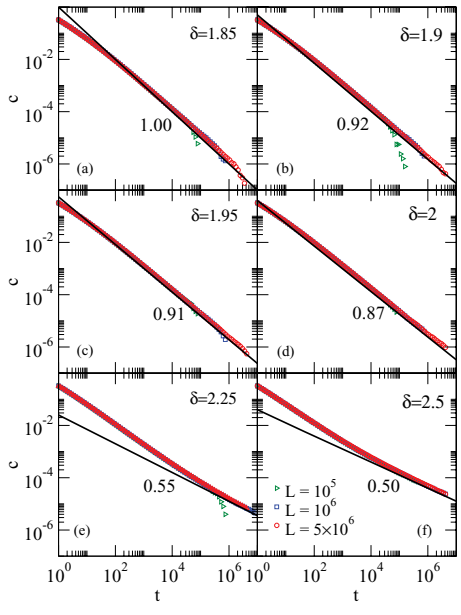

FIG. 5. (Color online) The concentration $c(t)$ of surviving particles in the case of annihilation, as function of time t for ER networks embedded in linear chains with $k = 4$, for the system sizes $L = 10^5$(green triangle), 10^6(blue square), and 5×10^6(red circle). The spatial exponents are $\delta = 1.85, 1.90, 1.95, 2, 2.25, 2.50$. For each parameter space we averaged over 50 configurations. For $d/d_w < 1$ the slopes of the straight lines have been taken from the predictions given in Fig. 3.

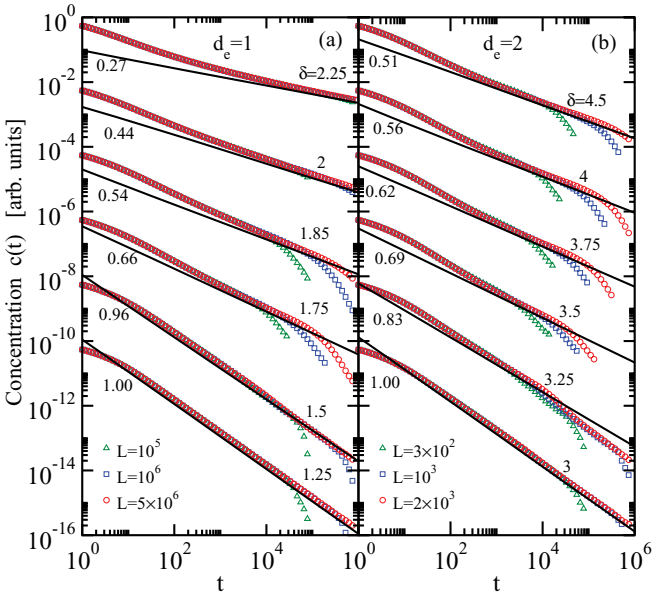

FIG. 6. (Color online) The concentration $c(t)$ of the surviving A or B particles in the chemical reaction $A + B \to C$ as function of time t for ER networks with $k = 4$ embedded (a) in linear chains ($d_e = 1$) of length $L = 10^5$(green triangle), 10^6(blue square), and 5×10^6(red circle) and (b) in square lattices ($d_e = 2$) of length $L = 3 \times 10^2$(green triangle), 10^3(blue square), and 2×10^3(red circle). The spatial exponents are $\delta = 1.25, 1.5, 1.75, 1.85, 2, 2.25$ in $d_e = 1$ and $\delta = 3, 3.25, 3.5, 3.75, 4, 4.5$ in $d_e = 2$. For each parameter set we averaged over 50 configurations. For $d/d_w < 2$ the slopes of the straight lines have been taken from the predicted values given in Fig. 3. For transparency, the 5 lower plots in each panel have been shifted vertically by 10^{-2} to 10^{-10}.

where C is some inert species irrelevant to the kinetics. For regular lattices of dimension d_e it is known that $c_A(t) = c_B(t)$ scales as $t^{-d_e/4}$ as long as $d_e \leqslant 4$ [21,22,24,35]. For $d_e > 4$, the concentrations decays as $1/t$. It is straightforward to generalize these results to the case of embedded networks with dimension d_e and diffusion exponent $1/d_w$,

$$c_A(t) = c_B(t) \sim \begin{cases} t^{-d/2d_w}, & d \leqslant 2d_w \\ t^{-1}, & d > 2d_w \end{cases}, \tag{9}$$

which reduces to the result for regular lattices described above, where $d_w = 2$ and $d = d_e$.

Accordingly, we can read from Fig. 3 how $c_A(t) = c_B(t) \equiv c(t)$ should decay with t. For $\delta < \delta_1 \cong 1.5\, d_e$ we expect that $c(t)$ decays as t^{-1}, while for $\delta > \delta_1$, $c(t)$ should decay as $t^{-d/2d_w}$. Figure 6 shows that this is indeed the case, both for $d_e = 1$ (a) and $d_e = 2$ (b). The straight lines in the figures have the predicted slopes obtained from Fig. 3. The crossover towards a stronger decay at very large time steps depends on the system size and, thus, is a finite-size effect.

VI. CONCLUSIONS

In summary, we considered Erdös-Rényi–type networks that are embedded in linear chains ($d_e = 1$) and square lattices ($d_e = 2$). We assumed that the link length distribution follows a power law, $p(r) \sim r^{-\delta}$. This is a realistic assumption since

many complex networks in space, like the global airline network or the Internet, have this link length power-law distribution [11,13]. It has been found [17] that for δ below d_e where the long links dominate, the spatial constraints are irrelevant; the network belongs to the universality class of Erdös-Rényi graphs and is characterized by an infinite dimension. For δ above $2d_e$, where the short links dominate, the network is in the universality class of regular lattices and its dimension is equal to the dimension d_e of the embedding lattice. In the intermediate regime between d_e and $2d_e$, the dimension decreases monotonously, from $d = \infty$ at $\delta = d_e$ to a value above d_e at $\delta = 2d_e$. Since in ordinary lattice-type systems with short-range links only, including fractal structures, the dimension is crucial for characterizing its physical properties like phase-transition phenomena and diffusion-driven chemical processes, we have tested here if this is the case for diffusion-driven annihilation and chemical reaction processes in spatially embedded networks. It is known that in regular and fractal lattices, the concentration of particles decays by a power law [24] where the exponent only depends on the ratio d/d_w, where d_w is the fractal dimension of the random walk. We have shown here that the dimension of the embedded network governs, in exactly the same way as for regular and fractal lattices, diffusion-driven annihilation and chemical reactions. Our results are only for Erdös-Rényi–type networks where the degree distribution is centered sharply around a maximum. It remains to be tested if the results are also valid for networks with a broad degree distribution, as for the scale-free Barabási Albert networks, where it was shown that for $\delta = 0$, $c(t)$ decays faster as t^{-1} [27,28].

ACKNOWLEDGMENTS

We gratefully acknowledge financial support from the Deutsche Forschungsgemeinschaft and the EPIWORK and LINC European Projects.

[1] R. Albert, H. Jeong, and A. L. Barabási, Nature **401**, 130 (1999).
[2] R. Albert and A. L. Barabási, Rev. Mod. Phys. **74**, 4797 (2002).
[3] M. E. J. Newman, D. J. Watts, and S. H. Strogatz, Proc. Natl. Acad. Sci. USA **99**, 2566 (2002).
[4] S. N. Dorogovtsev, *Evolution of Networks: From Biological Nets to the Internet and WWW* (Oxford University Press, Oxford, 2003).
[5] J. Goldberg and M. Levy, arXiv:0906.3202 (2009).
[6] R. Cohen and S. Havlin, *Complex Networks: Structure Robustness and Function* (Cambridge University Press, Cambridge, UK, 2010).
[7] R. P. Satorras and A. Vespignani, *Evolution and Structure of the Internet: A Statistical Physics Approach* (Cambridge University Press, Cambridge, UK, 2004).
[8] D. Liben-Nowell, J. Novak, R. Kumar, P. Raghavan, and A. Tomkins, Proc. Natl. Acad. Sci. USA **102**, 11623 (2005).
[9] D. Brockmann, L. Hufnagel, and T. Geisel, Nature **439**, 462 (2006).
[10] A. Barrat, M. Barthélmy, R. Pastor-Satorras, and A. Vespignani, Proc. Natl. Acad. Sci. USA **101**, 3747 (2004).
[11] A. Barrat, M. Barthélmy, and A. Vespignani, *Dynamical Processes on Complex Networks* (Cambridge University Press, Cambridge, 2008).
[12] R. Lambiotte, V. D. Blondel, C. de Kerchove, E. Huens, C. Prieur, Z. Smoreda, and P. Van Dooren, Physica A **387**, 5317 (2008).
[13] M. Barthélmy, Phys. Rep. **499**, 1 (2010).
[14] K. Kosmidis, S. Havlin, and A. Bunde, Europhys. Lett. **82**, 48005 (2008).
[15] Li Daqing, Li Guanliang, K. Kosmidis, H. E. Stanley, A. Bunde, and S. Havlin, Europhys. Lett. **93**, 68004 (2011).
[16] Li Daqing, K. Kosmidis, A. Bunde, and S. Havlin, Nat. Phys. **7**, 481 (2011).
[17] T. Emmerich, A. Bunde, S. Havlin, Li Guanlian and Li Daqing, arXiv:1206.5710 (2012).
[18] P. Erdös and A. Rényi, Publ. Math. Inst. Hung. Acad. Sci. **5**, 17 (1960).
[19] P. Erdös and A. Rényi, Publ. Math. Debrecen **6**, 290 (1959).
[20] B. Bollobás, *Random Graphs* (Cambridge University Press, Cambridge, UK, 2001).
[21] D. Toussaint and F. Wilczek, J. Chem. Phys. **78**, 2642 (1983).
[22] K. Kang and S. Redner, Phys. Rev. Lett. **52**, 955 (1984).
[23] L. Peliti, J. Phys. A **19**, L365 (1986).
[24] D. Ben-Avraham and S. Havlin, *Diffusion and Reactions in Fractals and Disordered Systems* (Cambridge University Press, Cambridge, UK, 2000).
[25] S. Havlin and D. Ben-Avraham, Adv. Phys. **51**, 187 (2002).
[26] D. Ben-Avraham and S. Redner, Phys. Rev. A **34**, 501 (1986).
[27] L. K. Gallos and P. Argyrakis, Phys. Rev. Lett. **92**, 138301 (2004).
[28] M. Catanzaro, M. Boguñá, and R. Pastor-Satorras, Phys. Rev. E **71**, 056104 (2005).
[29] J. M. Kleinberg, Nature **406**, 845 (2000).
[30] A. Bunde and S. Havlin (eds.), *Fractals and Disordered Systems* (Springer, Berlin, 1991).
[31] G. H. Weiss, *Aspects and Applications of the Random Walk* (North-Holland Press, Amsterdam, 1994).
[32] J. Klafter and I. M. Sokolov *First Steps in Random Walks* (Oxford University Press, Oxford, 2011).
[33] J. Klafter, M. F. Shlesinger, and G. Zumofen, Phys. Today **49**, 33 (1996).
[34] R. Metzler and J. Klafter, Phys. Rep. **339**, 1 (2000).
[35] K. Kang and S. Redner, Phys. Rev. A **32**, 435 (1985).